Development of an Ammonia-fueled Cracker-Engine-Unit as Propulsion System for Inland Waterway Vessels

Entwicklung einer Ammoniak-betriebenen Cracker-Motor-Einheit als Antriebssystem für Binnenschiffe

A. Braun[1], H. Kubach[1], S. Braun[1], M. Reinbold[1], S. Bernhardt[1], N. Gierenz[3], B. Buchholz[3], L. Engelmeier[4], L. Fehlemann[4], J. Plass [4], M. Steffen[4], T. Baufeld[2], S. Prehn[3], H. Mohr[5*]

[1] Karlsruhe Institute of Technology, Karlsruhe/Germany

[2] Liebherr Machines Bulle SA, Bulle/Switzerland

[3] University of Rostock, Rostock/Germany

[4] The hydrogen and fuel cell center ZBT GmbH, Duisburg/Germany

[5] GasKraft Engineering, Beckdorf/Germany

*Corresponding Author: hinrich.mohr@gaskraft-engineering.co

Abstract

Ships are an essential part of the global transport systems for goods and people. They represent the most efficient and climate-friendly transport method. However, a further reduction in emissions, especially CO_2, is necessary. Since pure electrification by using batteries as energy storage is not a solution in most cases due to the required operation range, the use of alternative fuels based on renewable energies is expedient. The CAMPFIRE partner alliance is therefore working intensively on the use of regeneratively produced ammonia as a maritime fuel and energy storage for regeneratively produced hydrogen. Due to the higher demand for hydrogen in the future, it will have to be imported and stored in ammonia for transportation. This will also increase the transport capacity required for inland shipping to distribute the energy from the seaports to the domestic market. Against this background, a project consortium of the CAMPFIRE partner alliance is developing and testing a propulsion system for inland vessels that runs exclusively on ammonia. The heart of this project is a cracker-engine-unit. During the work, the ammonia cracker is developed and built, the characteristics and challenges of ammonia combustion in the engine are systematically examined, the entire system is designed, the full engine unit with generator is containerized and finally tested holistically. In addition, the special safety aspects when using ammonia in the maritime environment are analyzed. The combination of the technologies used is intended to enable completely climate-neutral ship operations. The paper and presentation deal with an overview of the current work. This includes examples from the results of systematic combustion studies on the single-cylinder engine and the required injector technology. The various

configurations are evaluated for performance and emissions for a maritime application and then used as a basis for the full engine configuration. Furthermore, the development work on the cracker, which splits a partial stream of ammonia into hydrogen and nitrogen and thus supplies the ignition fuel for the engine, will be presented.

Kurzfassung

Schiffe sind ein wesentlicher Bestandteil der globalen Transportsysteme für Waren und Menschen. Sie stellen die effizienteste und klimafreundlichste Transportmethode dar. Dennoch ist eine weitere Reduzierung der Emissionen, insbesondere von CO_2, notwendig. Da eine reine Elektrifizierung durch den Einsatz von Batterien als Energiespeicher aufgrund der erforderlichen Reichweite in den meisten Fällen nicht in Frage kommt, ist der Einsatz von alternativen Kraftstoffen auf Basis erneuerbarer Energien sinnvoll. Die CAMPFIRE-Partnerallianz arbeitet daher intensiv an der Nutzung von regenerativ erzeugtem Ammoniak als maritimen Treibstoff und Energiespeicher von regenerativ erzeugtem Wasserstoff. Wegen der zukünftig größeren Nachfragen an Wasserstoff wird dieser importiert werden müssen und für den Transport in Ammoniak gespeichert werden. Damit wird u. a. auch die benötigte Transportkapazität in der Binnenschifffahrt steigen, um die Energie von den Seehäfen ins Landesinnere zu verteilen. Vor diesem Hintergrund entwickelt und erprobt ein Projektkonsortium ein Antriebssystem für Binnenschiffe, das ausschließlich mit Ammoniak betrieben wird. Das Herzstück dieses Projekts ist eine Cracker-Motor-Einheit. Im Rahmen der Arbeiten wird der Ammoniak-Cracker entwickelt und gebaut, die Eigenschaften und Herausforderungen der Ammoniakverbrennung im Motor systematisch untersucht, das Gesamtsystem ausgelegt, die komplette Motoreinheit mit Generator containerisiert und schließlich ganzheitlich getestet. Darüber hinaus werden die besonderen Sicherheitsaspekte beim Einsatz von Ammoniak in der maritimen Umgebung analysiert. Die Kombination der eingesetzten Technologien soll einen vollständig klimaneutralen Schiffsbetrieb ermöglichen. Das Manuskript gibt einen Überblick über die laufenden Arbeiten. Dazu gehören Beispiele aus den Ergebnissen systematischer Verbrennungsstudien zum Einzylindermotor und der erforderlichen Injektortechnologie. Die verschiedenen Konfigurationen werden hinsichtlich Leistung und Emissionen für eine maritime Anwendung bewertet und dann als Grundlage für die vollständige Motorkonfiguration verwendet. Außerdem werden die Entwicklungsarbeiten am Cracker vorgestellt, der einen Teilstrom von Ammoniak in Wasserstoff und Stickstoff aufspaltet und damit den Zündbrennstoff für den Motor liefert.

1. Introduction

Shipping is a major and irreplaceable means of transporting people and particularly goods worldwide. Ships provide the most efficient and therefore most climate friendly method of transport. However, further improvement of greenhouse gas emissions will be needed to cope with the requirements for a sustainable future. Potentially climate neutral mobility might be realized utilizing battery in road-based applications. For ships the energy densities of batteries are too low for most application scenarios [1]. In this respect alternative ways of providing stored renewable energies for ships are needed. Green hydrogen is a promising option for this task, but the energy density of elemental hydrogen (both, compressed or liquefied) is still too low. Conversion of hydrogen into a liquid fuel is therefore highly interesting. Classical hydrocarbons, that could be produced via e.g. the Fischer-Tropsch-process from hydrogen, seem attractive in this regard as conventional engines could be used. Of course, they require a concentrated carbon source e.g. from carbon capture and storage (CCS) plants, if no energy demanding and expensive direct air carbon capture is applied on a large scale. Consequently, the availability of CO_2 becomes a limiting factor for production capacities, which prohibits their wide-spread application [2]. In contrast, ammonia can be produced from hydrogen by conversion of hydrogen with abundantly available nitrogen [3]. So, ammonia has started drawing major attention by researchers as well as the maritime industry and authorities as a storage form for hydrogen and energy [4, 5]. Ammonia can be utilized directly in internal combustion engines as a fuel, but its combustion properties are not optimal for the engine process. Particularly its low ignitability and flame speed pose some challenges, especially for high-speed engines, as well as its potential corrosive attack [6]. Mixing with a certain amount of hydrogen as a pilot fuel can help to handle this issue [7]. The provision of this hydrogen could be facilitated by decomposition of a small share of the ammonia immediately before the engine in a cracker unit. To realize such a process in a reasonable manner, proper system integration is required. In this paper the application of ammonia as a fuel for inland water vessels is discussed by addressing the recent development topics.

2. System concept for inland water vessels

Inland shipping uses a large network of interconnected rivers, canals and lakes, primarily in Europe, North America and the Far East. The rather inconspicuous ships mostly transport dry and wet bulk goods as well as containers. Another expanding application is inland waterway transport with passengers. In addition to self-propelled monohull vessels, there are also push boats and tugs that move unpowered barges. Vessel sizes are often limited by the size of the lock basins, which allow the vessels a difference in height. These sizes are usually standardized in the respective regions. A typical size is the so-called European ship for European inland waters of class IV with a length of 85 m and a width of 9.5 m. The maximum transport capacity of this type of ship is 1350 tons. In 2020, the average age of German inland waterway vessels was 46.7 years [8].

Due to their smaller size and lower water resistance, the power requirement of inland waterway vessels is specifically lower than that of seagoing vessels, as the speeds are lower and there are almost no waves and winds to take into account. The highest power requirement is needed for upstream travel on rivers against the current. The so-called European ship type already mentioned has a typical power requirement of 600 kW. In the past, this was handled by a medium-speed engine that drove a single propeller with a fairly large diameter via a reduction gear. As river water levels have been low more frequently over the last decade due to low rainfall in Europe, new vessels are being designed with two or even three smaller diameter propellers to reduce the draft of the vessel. These smaller propellers are driven mechanically by high-speed engines via a Z-drive or electrically via a generator. Naturally, a lower water level greatly increases the power requirement for a European ship type (see Table 1). With the

same performance, the ship's speed is reduced to 50% if the water level is lowered from 5 m to 2.5 m and the draught is limited to 2 m.

Table 1: Influence of water level on ship speed @ constant engine power [9]

Engine Power / kW	Water Level / m	Ships Draught / m	Ship Speed/ km/h
600	5	2.5	17
600	2.5	2	8.5

In order to drive forward the decarbonization of shipping, the CAMPFIRE project CF08_2 is developing an ammonia-powered, containerized inland vessel propulsion system with 350 kW propulsion power and testing it “on land”. Figure 1 shows a schematic overview of the propulsion system. To improve the ignition and efficient conversion of the ammonia in the engine, a low amount of hydrogen is required as ignition improver. For this purpose, an ammonia cracker is connected upstream of the engine, which decomposes a partial flow of the ammonia into hydrogen and nitrogen and feeds this mixture to the combustion engine.

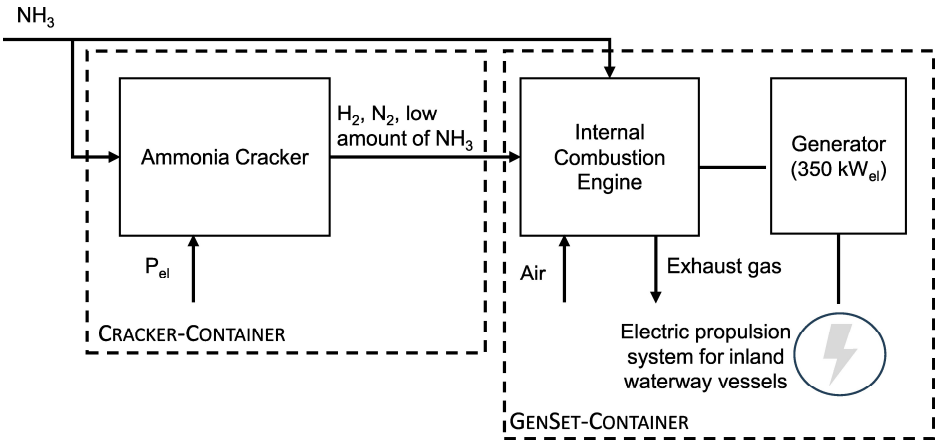

Figure 1:Scheme of the ammonia-powered propulsion system of an inland waterway vessel

3. Methodology of Development

3.1. Internal Combustion Engine

The development of a new combustion process involves uncertainties and, due to the novelty of ammonia as a fuel, a lack of both experience and validated tools. The development process therefore includes both expected and unexpected challenges. The expected challenges are mainly due to the chemical properties of ammonia. On the one hand, the rather poor combustion properties as described in the previous chapters, and on the other hand, the possible incompatibility of materials. Other known challenges include the lack of validated simulation tools that would allow rapid refinement and validation of new concepts. Examples of the lack of experience include atomization, evaporation and mixing behavior, combustion behavior, and heat release of ammonia. In the case of conventional fuels, there is a wealth of experience in terms of appropriate modeling. To achieve the ultimate goal of developing a combustion process for a multi-cylinder engine, the following strategy is used (Figure 2). A single-cylinder engine is used to test the basic concepts. The extensive instrumentation of this research engine allows the determination of the calibration quantities required for the essential 0D/1D simulations. The models validated on the single-cylinder engine are then used for the process development of the multi-cylinder engine. Certain quantities that cannot be measured directly are determined using detailed 3D flow simulations. These quantities are then fed into the 0D/1D tools. The final step is to apply the knowledge gained from the single-cylinder test bench and the validated 0D/1D models to the complete engine. The experimental work on combustion process development is carried out in Karlsruhe on a single-cylinder engine

derived from the Liebherr multi-cylinder diesel engine. The multi-cylinder engine tests will be carried out in Rostock by the University of Rostock.

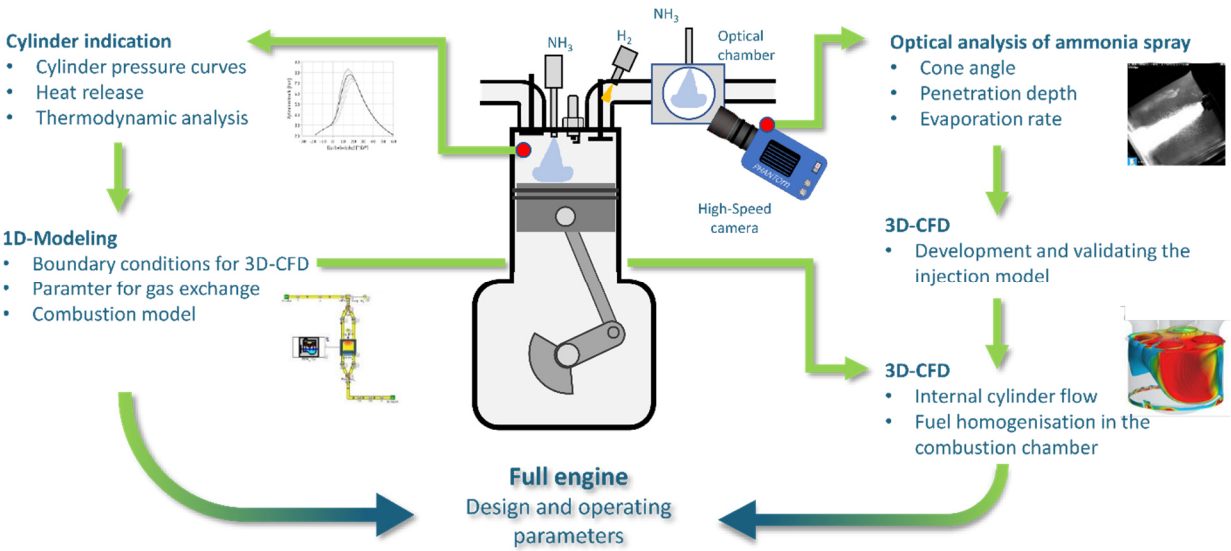

Figure 2: Development methodology for the combustion process

3.2. Cracker

In order to supply the required amount of hydrogen to the engine, a certain share of the ammonia feed has to be decomposed into hydrogen by the use of a suitable process. The decomposition into hydrogen and nitrogen is often referred to as ammonia cracking and is an endothermic process with a reaction enthalpy of about 46 kJ/mol. The reaction equation without intermediate steps can be seen in equation (1) [10].

$$NH_3 \leftrightarrow \frac{1}{2}N_2 + \frac{3}{2}H_2 \qquad \Delta H^0 = +45{,}9\ kJ/mol \qquad (1)$$

Figure 3 shows the equilibrium ammonia mole fraction as a function of temperature at pressures of 1 bara, 5 bara and 10 bara. In accordance with Le Chatelier's principle, the equilibrium shift can be achieved by increasing temperature or reducing pressure.

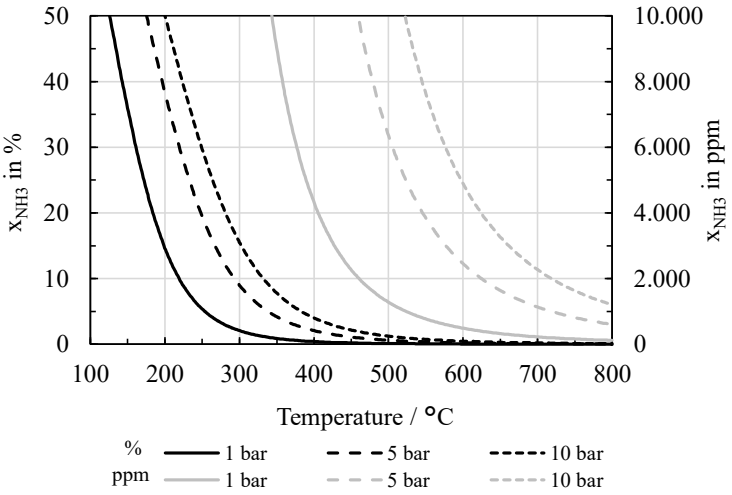

Figure 3: Simulated equilibrium ammonia mole fraction as a function of temperature at a pressure of 1 bara, 5 bara and 10 bara, simulated with Aspen Plus®

In practice, the chemical equilibrium shown in Figure 3 is not achieved due to kinetic limitations, especially at low temperatures. Thus, in order to provide hydrogen in a sufficient amount both a *catalyst* and *higher temperatures* (up to 900 °C) are required.
As such, the development of the ammonia cracker starts with the identification and selection of a suitable catalyst. For this purpose, various catalysts are procured and extensively tested with regard to their conversion as a function of temperature, gas hour space velocities and pressure as well as long-term stability. Focus lies on monolithic catalysts (ceramic and metallic), as these are particularly advantageous when vibrations in mobile applications cause abrasion in bulk catalysts [11].
Preliminary investigations have shown that the conditions in an ammonia cracker, characterized by the combination of high temperature and an ammonia-rich atmosphere, lead to considerable material damage due to nitridation. The next step is therefore the selection of an appropriate reactor material. Promising material candidates are thus identified in an extensive literature survey. Subsequently, long term exposure tests are carried out to verify the suitability of the selected materials.
Based on the properties of the carefully chosen catalyst and reactor material as well as according to the requirements set by the engine the ammonia cracker is developed, focusing on an optimized heat integration and thus high efficiency. Aspen Plus® is used to model and compare different possible process designs, as well as to determine energy and material flows, necessary for engineering the ammonia cracker components such as reactor, heat exchangers, burner, compressors etc. The detailed engineering of the single components is supported by multiphysics simulations (COMSOL Multiphysics®) as well as FEM simulations (Nastran, Autodesk Inventor). This is followed by the engineering and construction of the ammonia cracking plant, comprising the ammonia cracker, balance of plant components, rack, enclosure including an appropriate control system (SPS). The ammonia cracking plant is being put into operation at the ZBT and is extensively tested and optimized. The plant will then be containerized and transferred to Rostock to be coupled with the engine for extensive testing of the entire system. Both initial characterization at ZBT as well as subsequent tests in Rostock will be used for process optimization aided by dynamic process simulations in AVL Cruise™ M.

4. Results

4.1. Single-cylinder Engine

A single-cylinder research engine was built on a test bench at the Institute of Internal Combustion Engines at KIT. The engine is based on a Liebherr D966 diesel engine and was modified to meet the requirements of the new combustion process. The Diesel injector was replaced by an injector that can inject both hydrogen and ammonia in liquid and gaseous form. As ammonia has a very low calorific value of only 18.8 MJ/kg compared to diesel fuel, the injection system must be designed for comparatively large mass flows in order to achieve diesel-like mean pressures. As this combustion process is a spark-ignition principle, a spark plug must also be integrated into the cylinder head. In addition to the possibility of direct injection, both media can also be injected into the intake manifold. The test bench was equipped with a suitable fuel infrastructure for this purpose. While hydrogen is already available in cylinders at a pressure of 300 bar, the ammonia, which is also available in cylinders, is brought to the desired injection pressure of up to 30 bar via a compressor station. Dual-fuel operation with ammonia and hydrogen is necessary at most operating points, as ammonia is difficult or impossible to ignite with a conventional spark plug and has slow combustion rates [12]. Hydrogen supports the ignition process and ensures a higher burning rate. On the other hand, the high enthalpy of vaporization of ammonia can bring advantages. For example, the cooling effect could suppress knocking combustion and reduce nitrogen oxide emissions. The development goal is to operate the engine with as little hydrogen as possible while maximizing efficiency and reducing emissions. As the hydrogen is provided by the aforementioned cracker, it can then be built as small and cost-effective as possible and operated with low energy consumption. In this study, operating limits for the maximum and minimum hydrogen content are to be determined for the single-cylinder engine when the

ammonia is injected into the intake manifold in liquid form and the hydrogen in gaseous form. The main limiting factors are the occurrence of knocking combustion or pre-ignition, excessive variance in the mean pressure and exceeding the permissible exhaust gas temperature and permissible peak pressure.

Table 2: Engine parameters

Cylinder	1
Stroke	157 mm
Bore	135 mm
Compression ratio	14
Max. speed	1900 rpm
Operating principle	4-stroke
Displacement	2.24 l
Type	Modified Liebherr diesel engine

4.1.1. Injection timing

The homogenization of the cylinder charge can be significantly influenced by the injection timing. The hydrogen is injected at the start of injection at SOI = 330 °CA bTDCf and is already in gaseous form. The ammonia must first evaporate and mix with the hydrogen and the air in the combustion chamber. The influence of the start of injection of ammonia is investigated in three steps by varying the ammonia/hydrogen ratio. Starting at SOI = 130 °CA bTDCf, the ammonia is injected shortly after IVC and thus has the maximum time span to evaporate before IVO. A significant proportion of the vaporization can thus already take place in the intake port. Due to the very high enthalpy of vaporization, there is significant icing on the outside of the intake manifold. In the second step, injection begins at SOI = 265 °CA bTDCf, synchronized with the intake at maximum open IV. In the last variant at SOI = 360 °CA bTDCf, injection begins shortly after IVO (403 °CA bTDCf).
Figure 4 shows the coefficient of variation (COV) of the indicated mean effective pressure (IMEP) over the energetic ammonia content for the three injection timings mentioned. The series of measurements was carried out at IMEP = 17 bar, which corresponds to a power output of 44 kW. The upper limit value results from exceeding a COV of 3%. At SOI = 360 °CA bTDCf, this is the case with an energetic ammonia content of approx. 83%. If the ammonia content is increased further, the COV gradients for all SOI increase very sharply, so that stable engine operation is no longer possible. For this reason, no further increase was made.
In all three cases, the lower limit results from the occurrence of knocking combustion. Over the entire course, the IMEP shows the lowest cyclical fluctuations with intake-synchronous injection (SOI = 265 °CA bTDCf). Apparently, this injection start leads to the best mixture preparation and stabilization of combustion.

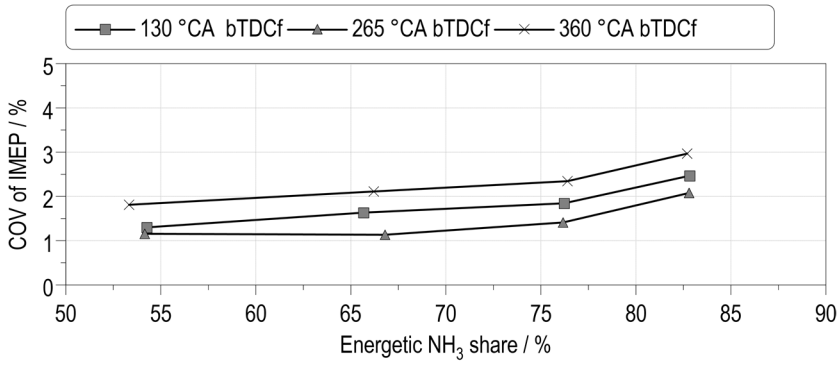

Figure 4: Influence of the ammonia start of injection timing on the COV of IMEP

4.1.2. Influence of the charge air temperature

In addition to the injection timing, the charge air temperature also has an influence on the mixture formation and thus the combustion stability, but also on the ignition behavior and thus on the occurrence of knocking events. To evaluate this influence, the charge air temperature was set to 40 °C, 60 °C and 80 °C. As in the previous chapter, the coefficient of variation of the indicated mean effective pressure over the energetic ammonia content up to approx. 83% is shown in Figure 5. A comparison of the two boundary values 40 °C and 80 °C shows the expected effect with high ammonia contents. The increased charge air temperature supports evaporation and mixture formation and stabilizes combustion, which is reflected in a reduced COV. The opposite effect occurs in the direction of lower energetic ammonia content. Here, the high temperature has a negative effect on knocking behavior. Increased knocking events worsen the COV here and lead to an interruption of operation with higher ammonia proportions and correspondingly less hydrogen. Since high hydrogen contents due to heavy knocking and pre-ignition represent the critical limit in terms of damage, especially at full load, the charge air temperature of 40 °C was initially selected for the further series of measurements for safety reasons.

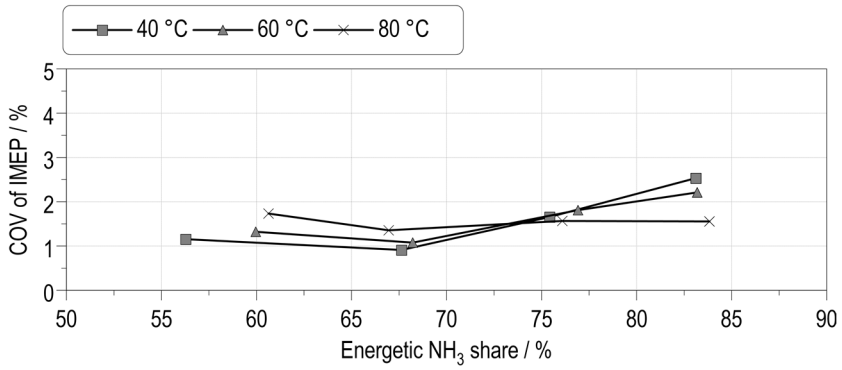

Figure 5: Influence of the charge air temperature on the COV of IMEP

4.1.3. Load Variation

The target speed of the final engine application is 1,500 rpm. The engine must be able to cover the entire load range. For this reason, a load sweep is analyzed at this speed with four steps in IMEP: 6.3 bar (25%), 11.5 bar (50%), 17 bar (75%) and 22 bar (100%). In this investigation the start of injection for ammonia is set to 130 °CA bTDCf and a charge air temperature of 40 °C is set. At this point, SOI = 130 °CA was chosen because optical investigations of the ammonia injection are also available here, which can be used for further interpretation of mixture formation effects. The initial focus is on the question of the range in which the energetic ammonia content can be varied depending on the load and what limits this range. Furthermore, it should be clarified how the emissions and efficiency depend on the selected ammonia proportion.

Figure 6 shows the IMEP, Lambda, the COV, as well as the center of combustion (AI50%) with the associated ignition timing for the different load levels. The maximum load corresponds to an effective output of 60 kW. This even slightly exceeds the desired target value of at least 57 kW. The load ranges 50% to 100% were run with a stoichiometric air/fuel ratio. As the engine does not have a throttle, the air ratio increases to Lambda=2.5 at 25% load. Since it is not trivial in test operation to keep the load exactly constant when changing the hydrogen/ammonia proportion and the associated change in the combustion process, small changes can be seen both in the load and in the air ratio (especially at 25% load, since the load is directly related to the air ratio here). The center of combustion was set to about 10 °CA aTDC as a compromise between the best possible efficiency and slightly reduced knocking tendency at high hydrogen percentages, since the engine has a high compression ratio for hydrogen operation with Epsilon = 14.

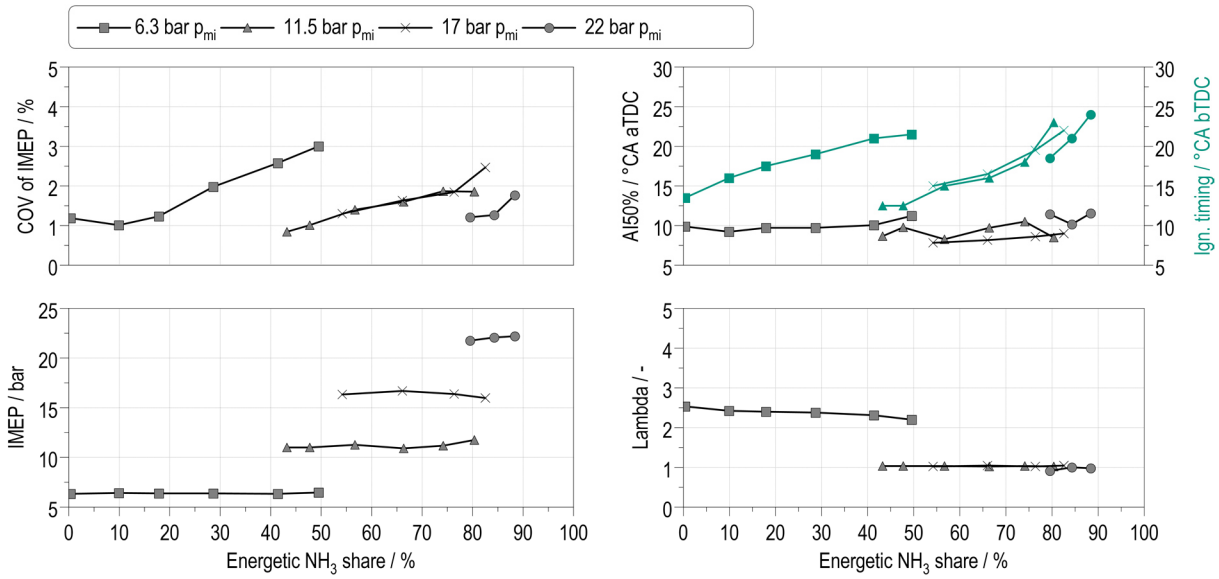

Figure 6: COV of IMEP, AI50, ignition timing, IMEP and Lambda at load variation

Pure hydrogen operation without combustion anomalies is possible with a low load and high air ratio. If the ammonia content is increased, the COV initially rises continuously up to an ammonia content of 50%. The gradient then increases significantly, and the cyclical fluctuations increase to such an extent that useful engine operation is no longer possible. At higher loads, no such sharp increase in running unsteadiness can be seen. However, if the ammonia content is increased further at loads above 25%, combustion misfires occur directly, so that engine operation is no longer possible. On the other hand, pure hydrogen operation is no longer possible at these loads. The lower limit of the ammonia content results here from a sharp increase in knocking combustion. If the ammonia content is lowered further, spontaneous pre-ignition occurs, resulting in extreme knocking and peak pressure overshoot. In Figure 7 left, 200 cylinder pressure curves for maximum hydrogen content (21% energetic) are shown for full load. In some cycles, very noticeable knocking already occurs. The maximum pressure amplitudes exceed 12 bar. If the hydrogen content is increased even slightly further, the knocking increases extremely and pre-ignition occurs. As a measured value recording takes approx. 30 seconds, this was not carried out for reasons of engine protection. Figure 7 on the right shows that individual cycles with very low peak pressures and very late combustion already occur at the upper limit of the ammonia content (88% energetic). With a further increase in the ammonia content, complete combustion misfires then occur, which no longer permit useful engine operation.

As mentioned in the introduction, the center of combustion was set to around 10 °CA aTDC. If the ammonia content is increased, this results in an increased spark advance requirement. This is plausible, as ammonia itself can hardly be ignited with a conventional spark plug as used here. Hydrogen is used for this purpose and to increase the flame speed. After ignition and with increasing temperature, ammonia decomposes into nitrogen and hydrogen, which further accelerates the flame speed and the heat release rate and thus the decomposition of ammonia [12]. After a longer ignition phase, a self-reinforcing acceleration effect of the flame speed can occur, so to speak.

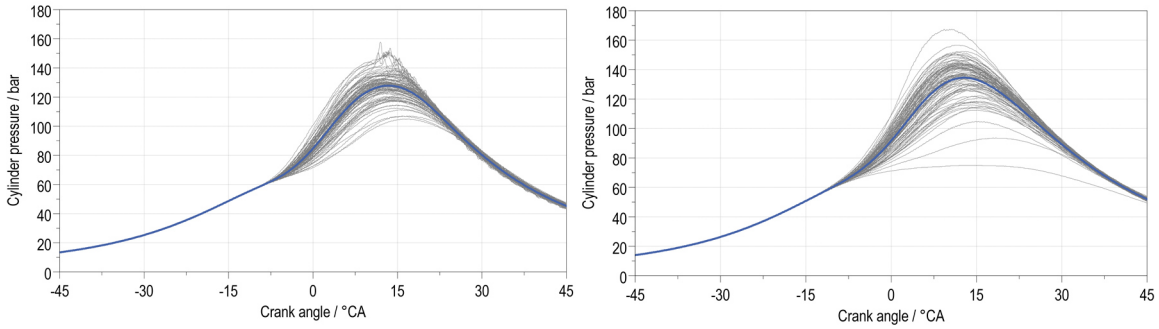

Figure 7: Cylinder pressure of a 100% load point with minimum (left) and maximum (right) amount of NH_3, averaged cylinder pressure in blue

As can be seen in Figure 8, the efficiency increases noticeably with the load. At 22 bar, there is only one measuring point, as with a higher NH_3 content and correspondingly lower H_2 mass flow, the latter was below the measuring limit of the Coriolis flow meter. What was not initially expected is the fact that the efficiency also tends to increase with the ammonia content. However, this statement is also supported by the drop in exhaust gas temperature, which indicates an increase in efficiency at constant load. The detailed analysis of the combustion behavior and the resulting effects on efficiency and emissions is the subject of ongoing investigations. The exhaust gas temperature is already in the limit range from 50% load on. With regard to the thermal stability of the cylinder head, 650 °C must not be exceeded here. The maximum peak pressure, on the other hand, whose limit value is 220 bar, is not critical at any load point. However, if pre-ignition occurs when the hydrogen content is slightly too high, it may well be exceeded. Therefore, such combustion anomalies must be avoided in all cases by maintaining a suitable distance from the corresponding limit value for the critical hydrogen concentration.

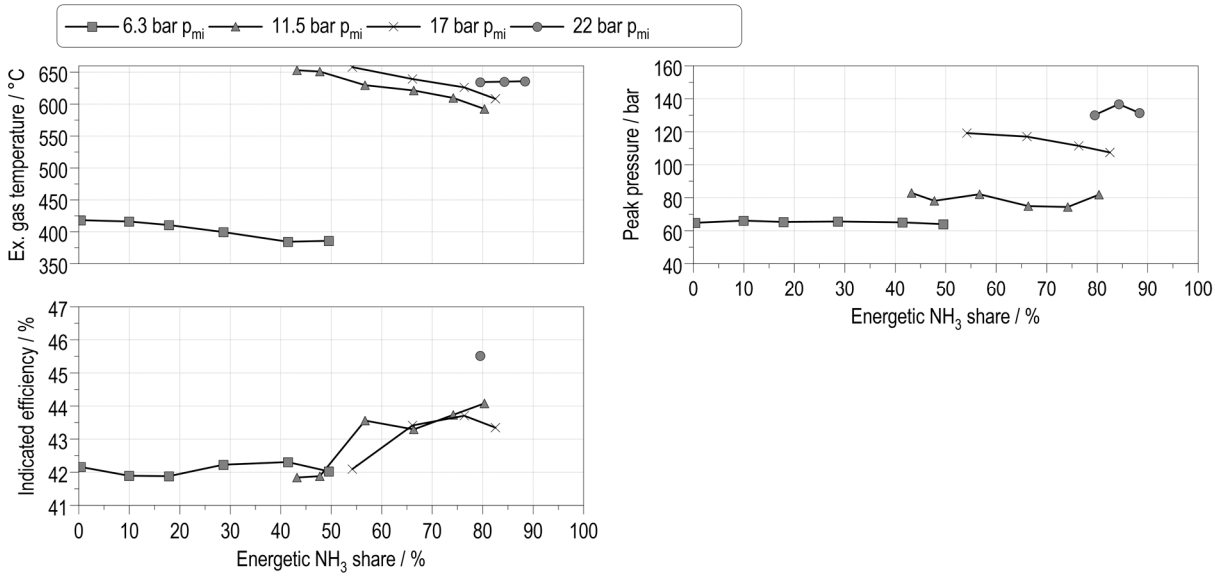

Figure 8: Exhaust gas temperature, peak pressure and indicated efficiency

In summary, the limits for the maximum ammonia content and the latter are shown in Figure 9. The following limits were set: Exhaust gas temperature = 650 °C, COV IMEP = 3%, maximum cylinder pressure = 220 bar. Only at a load of 25% does COV IMEP clearly reach an abort criterion. As already mentioned, the exhaust gas temperature is close to the limit value and the peak pressure is not critical. At loads higher than 25%, there is an abrupt transition from moderate COV IMEP below the limit value to operation that is no longer free of misfires and thus to termination.

The minimum ammonia content and thus the maximum hydrogen content always result from the occurrence of knocking and pre-ignition, apart from the 25% load point.

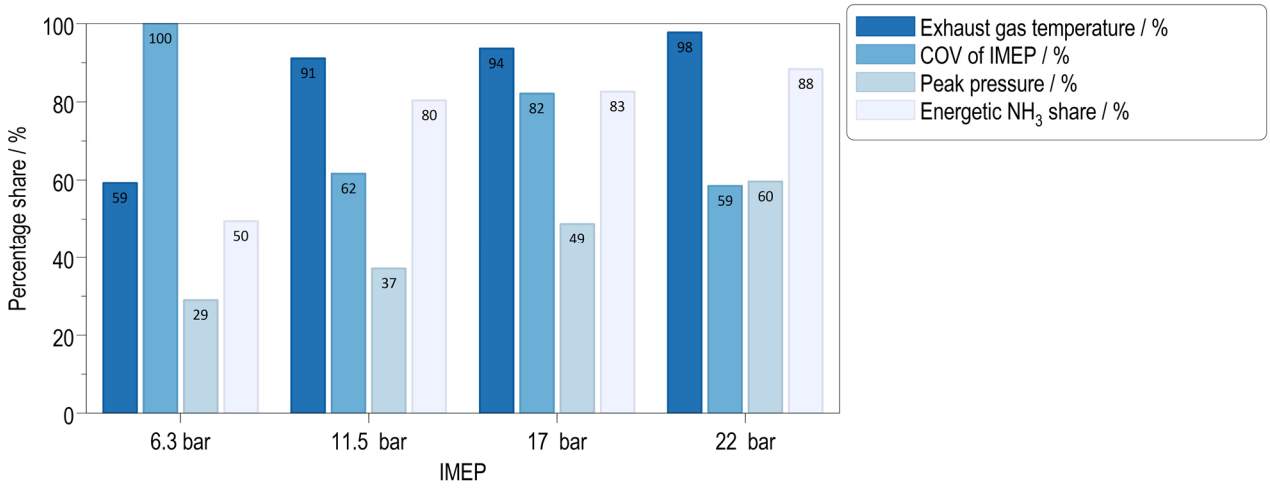

Figure 9: Termination criteria for the further substitution of ammonia for each load point

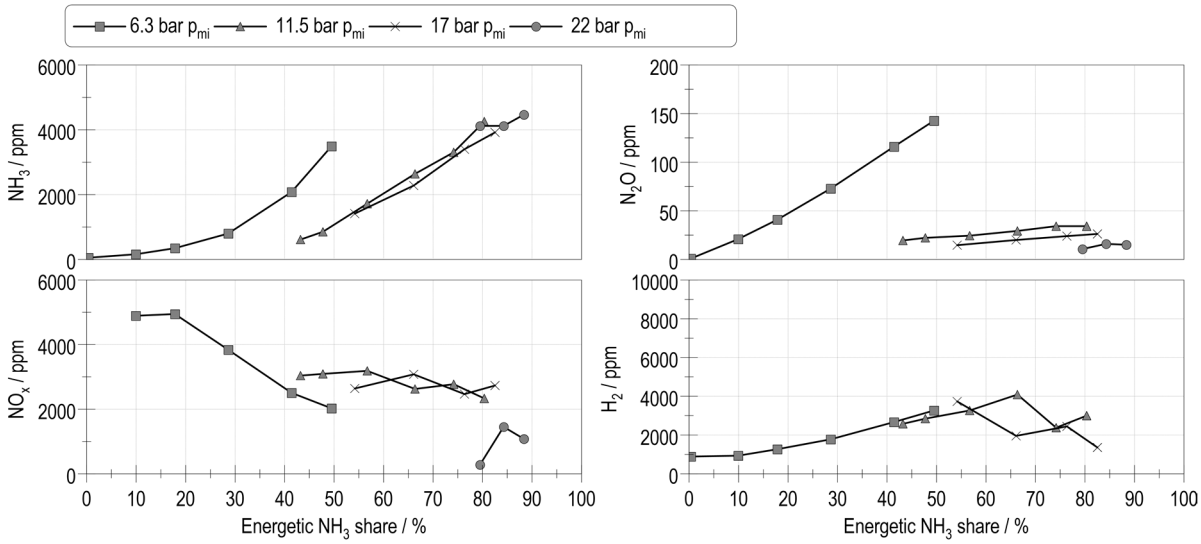

Figure 10: NO_x-, NH_3, N_2O and H_2-Emissions of the ammonia-hydrogen-combustion process

Figure 10 shows the most important emissions. In Lambda=1 operation, NH_3 emissions increase almost linearly with the ammonia content. The peak values for the ammonia slip are between 4,000 and 4,500 ppm, irrespective of the load. At a load of 6.3 bar IMEP and lean operating mode, ammonia emissions even increase almost exponentially from zero and reach a maximum of approximately 3,800 ppm. This is also where the highest N_2O emissions occur at 150 ppm. At higher loads, the dependence on the NH_3 content is negligible and the values are in the lower two-digit ppm range. The NO_x reaches its peak value of 5,000 ppm at the lowest load and low ammonia content, respectively at high H_2 content. As the ammonia content increases further, the NO_x decreases to 2,000 ppm. At higher loads, no such dominant dependence of the NO_x concentration in the exhaust gas on the NH_3 content in the fuel is evident. In combustion engines with conventional fuels, nitrogen oxide formation is mainly caused by atmospheric nitrogen according to the Zeldovich mechanism. In this case, so-called fuel-NO can be formed at temperatures as low as 800 °C via the formation of intermediate products such as hydrocyanic acid (HCN) and hydrazine (NH_n), especially if hydrogen is present at the same time, and may explain the high nitrogen oxide emissions in the exhaust gas even at low load and high air ratio. The values for 11.5 and 17 bar IMEP are all between 2,000 and 3,200 ppm. The lowest values occur at maximum load and are well below 2,000 ppm. The hydrogen slip increases significantly and steadily with the ammonia content at the lowest load until the peak value of around 3,500 ppm is reached. At the two medium loads, no

continuous dependence is recognizable. At 50% load, the NO_x is between 2,000 and 4,000 ppm and tends to be constant at 3,000 ppm on average. At 75% load, a decrease can be seen with increasing ammonia content from 4,000 to below 2,000 ppm. It is possible that the relatively high hydrogen emissions result from flame quenching effects caused by the cooling due to the high enthalpy of vaporization of the ammonia.

4.2. ICE Simulation

The 0D/1D model is generated using the GT-Power software package from Gamma Technologies. This software tool is widely used in the automotive and engine industries.

In addition to modelling the engine parts and piping, various combustion models can be set to simulate NH_3/H_2 combustion. In the current investigation, the predictive SI-Turb model is used, which is preferred for spark-ignited engines. A key element of this two-zone model is the calculation of the combustion velocity by determining the flame front velocity. This flame front velocity is divided into a laminar and a turbulent velocity. For conventional fossil fuels, the laminar flame velocities can be obtained from a library. For blends of non-carbon fuels, however, further development was required. The basis for this data is adapted from [14].

The turbulent flame velocity formula consists of several multipliers that need to be calibrated using the previously collected measurements. Before this calibration process can begin, the engine model must be correctly constructed. A key aspect of the engine flow model is the correct modelling of the cylinder head. For example, the intake and exhaust ports cannot be represented by individual short pipes due to their complexity, so they are modelled using a discharge coefficient sub-model.

Reliable determination of discharge coefficients has a huge impact on the accuracy of 0D/1D simulations used in the engine design and optimization process. Based on these coefficients, the 1D model calculates the cylinder charge and the trapped mass after gas exchange. Traditionally, charge coefficients are determined by evaluating a large number of measurements using a stationary flow bench. Since it is not possible to subject the engine head to the experimental setup, a virtual version of the flow bench was developed using the commercial software CONVERGE and used for the investigation. TECPLOT 360 was used to analyze the results.

4.2.1. Virtual Flowbench Simulation with 3D-CFD

Theory

A discharge coefficient describes the ratio of the isentropic flow cross-section to the reference valve cross-section.

$$\alpha_V = \frac{A_{is}}{A_V} \tag{2}$$

Isentropic flow does not include friction or other hydrodynamic effects. In combination with the isentropic velocity and density (c_{is} and ρ_{is}) the mass flow can be derived.

$$\dot{m} = A_{is} \cdot c_{is} \cdot \rho_{is} \tag{3}$$

Isentropic velocity can be determined as follows.

$$c_{is} = \sqrt{\frac{2 \cdot \kappa}{\kappa - 1} \cdot R_{air} \cdot T_1 \cdot \left(1 - \left(\frac{p_2}{p_1}\right)^{\frac{\kappa-1}{\kappa}}\right)} \tag{4}$$

Where T_1 and p_1 are the temperature and pressure far upstream of the valves, p_2 is the cylinder pressure, R_{air} is the gas constant of air, and κ is the specific heat ratio of air.
Isentropic density can be derived with the density ρ_1 far upstream, the pressure ratio and specific heat κ.

$$\rho_{is} = \rho_1 \cdot \left(\frac{p_2}{p_1}\right)^{\frac{1}{\kappa}} \tag{5}$$

A more detailed description of the dependencies and assumptions can be found in [14].

The swirl and tumble generated during the intake stroke has critical effects on the cylinder charge and mixing behavior in the cylinder. To capture these effects in the 0D/1D model, additional swirl and tumble coefficients for the intake valves are required. Based on the software provider of the 0D/1D model, the following calculation method is used for the swirl coefficient, where M_S is the angular momentum flux in the swirl direction and B is the bore of the cylinder [15].

$$C_S = \frac{2 \cdot M_S}{\dot{m} \cdot u_{is} \cdot B} \tag{6}$$

The calculation of the tumble coefficient is similar to the angular momentum flux in tumble direction.

Model Setup and Results

The geometry of the virtual flow bench consists of the intake port, exhaust port, and cylinder of the engine, combined with relaxation zones to ensure numerical stabilization of the simulation. In order to study the intake valve flow from the inlet to the cylinder (defined as the downstream direction), the liner was enlarged to a length of 2 times bore. In addition, the piston was removed and replaced with a circular plane in all models. To study the backflow from the piston to the inlet (defined as the upstream direction), the inlet port was also extended with a relaxation vessel for a numerically stable simulation. The same methods were applied to the simulation models of the exhaust valve studies. As mentioned earlier, additional swirl and tumble coefficients are needed for the downstream simulations of the intake valve. For this, a region approximately 0.5 times bore vertical distance from the cylinder head is used to calculate the angular momentum flux. The four geometries for the numerical investigations are shown in Figure 11.

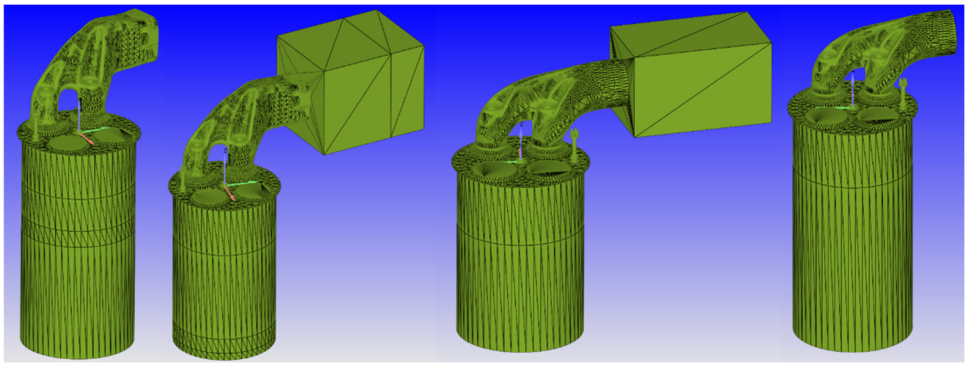

Figure 11: Geometries for the virtual flow bench

A steady-state solver with the PISO algorithm is used to compute the results. For turbulence modeling, the k-eps URANS is used. To ensure mesh independence of the numerical results, five different meshes were generated with base sizes ranging from 16 mm to 8 mm. All meshes generated include scale 2 refinements at the valves and valve seats to ensure that all flow phenomena are captured. In addition, the mesh around the surfaces is refined with fixed embeddings at scale 6. The intake and exhaust ports and the cylinder walls are refined at a scale of 4. Figure 12 shows the 16 mm and 8 mm meshes, both with a valve lift of 1.5 mm.

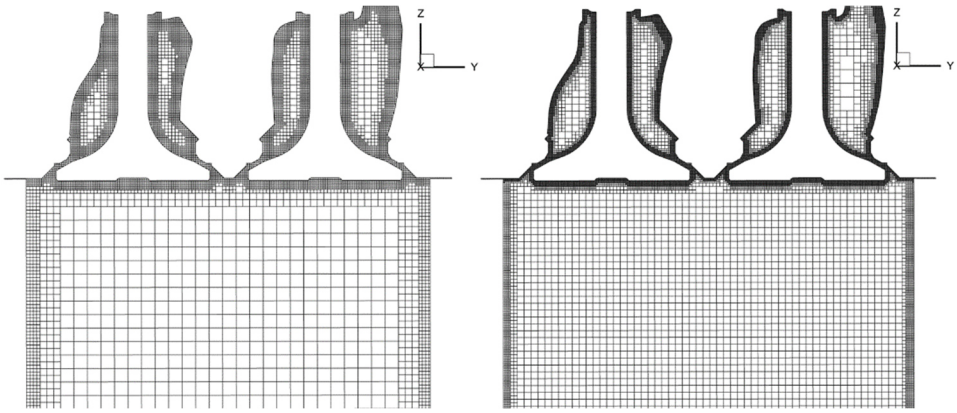

Figure 12: Lateral slices of the cylinders, coarsest (left) and finest mesh investigated

The mesh independence study simulations were all performed with 1.5 mm valve lift, as this is where the highest velocities and therefore the most complex flow phenomena occur. The following Table 3 lists the characteristics and results of the mesh independence study simulations.

Table 3 Values of mesh independence study

Base Size [mm]	Cell Count [mio.]	Mass Flow [g/s]	Deviation [%]
16	1.57	41.9942	-
14	2.08	41.2042	1.88
12	2.81	40.8229	0.93
10	4.21	40.8282	-0.01
8	6.64	40.9369	-0.27

As can be seen in Table 3, when using a 12 mm mesh, the deviation is already less than 1% compared to 14 mm. For further investigations, a base mesh size of 10 mm was chosen. To prove the pressure independence of the results, 1.5 mm lift simulations with 40 mbar to 90 mbar pressure drop between inlet and outlet boundary conditions were set up. Figure 13 shows the dependence of the flow coefficient on the pressure drop.

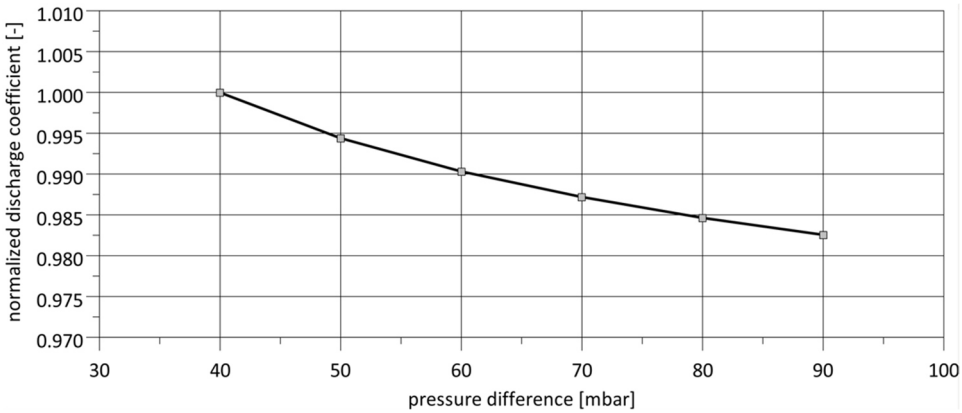

Figure 13: Normalized discharge coefficient over pressure difference

Figure 13 illustrates that as the pressure difference increases, the relative change in the discharge coefficient becomes smaller. Larger pressure differences result in higher velocities and higher computational costs. This is because smaller time steps are required during the calculation to reach the CFL criterion. Since the change in the discharge coefficient at 70 mbar compared to the 60 mbar version is -0.32% and the computational effort is still acceptable, 70 mbar pressure difference is used for the investigations. The independence of the results from the pressure difference is approximately confirmed.
Using a pressure difference of 70 mbar and 4.21 million cells, a simulation with a total wall clock time of 2 hours and 14 minutes was successfully completed. This performance was made possible by the parallel processing capability of 3 nodes with 76 cores each on a high-performance computing system.

4.2.2. 1D-Engine Modell

The relevant variables for the creation of the discharge coefficients were the valve lift, the mass flow through the cylinder ports, the upstream temperature and the physical properties of the used gas.
By applying the formulas (2-4) the following discharge coefficients can be calculated (see Figure 14).

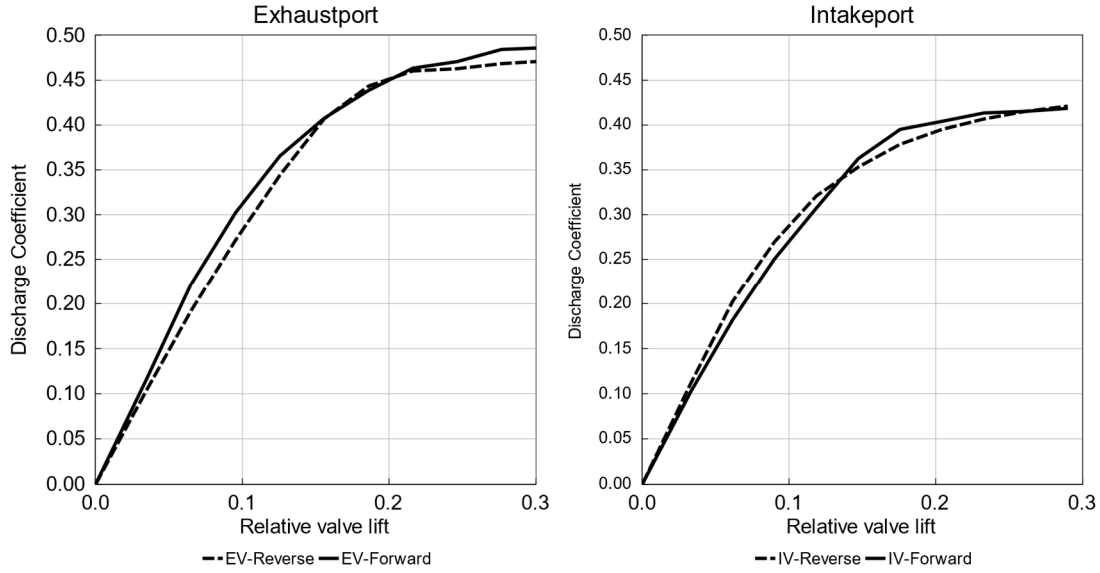

Figure 14: Calculated discharge coefficients for Intake (left) and exhaust ports (right)

Although the coefficients represent the flow well, there are still uncertainties regarding the heat transfer from the cylinder head to the charge air. This can be considered by a heat transfer model, which needs to be calibrated due to insufficient input data about the cooling flow around the intake and exhaust ports. The resulting heat transfer has a large impact on the volumetric efficiency of the engine. To calibrate this heat-transfer coefficient, a variety of motoring curves have been measured. Figure 15 shows the variation of engine speed and load respectively charge air pressure.

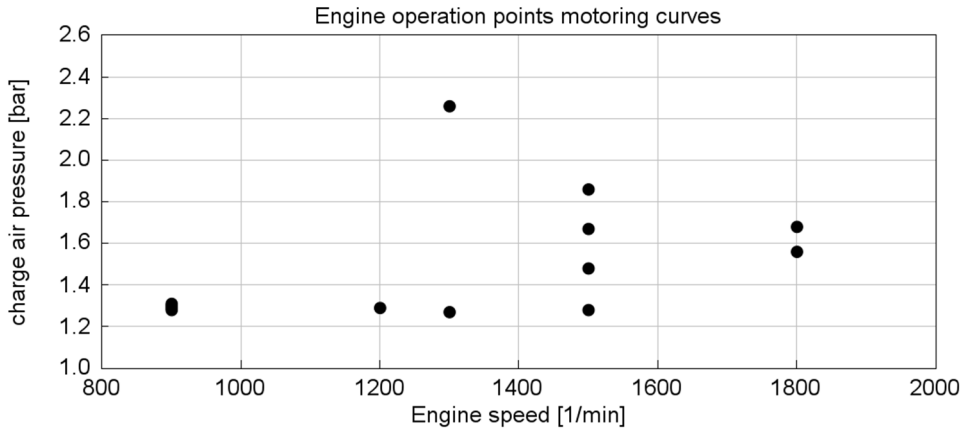

Figure 15: chosen engine operating points of the motoring curves

After the calibration has been conducted, a comparison between the measured and the simulated air masses in the cylinder is shown in Figure 16. It can be stated that the simulated air masses differ from the measurements within a 3% confidence band. The overall average error is -0.28% which is satisfying regarding the occurring normal measurement errors.

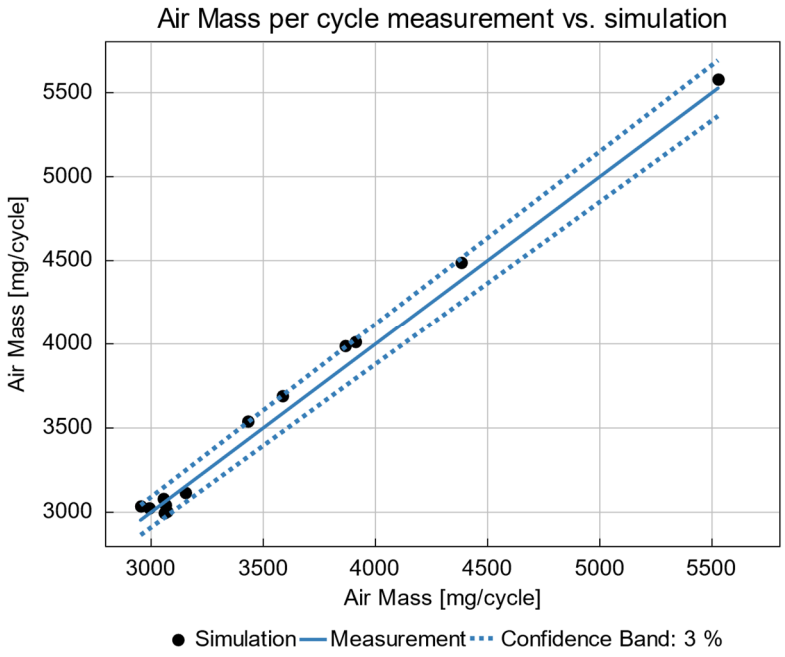

Figure 16: comparison of simulated and measured air masses per engine cycle

The resulting motoring pressure curve of a chosen operating point can be seen in Figure 17. It shows a good match between the simulation and the measurement data. With the correct cylinder head multipliers, the calibration of the combustion model can be carried out in a following step.

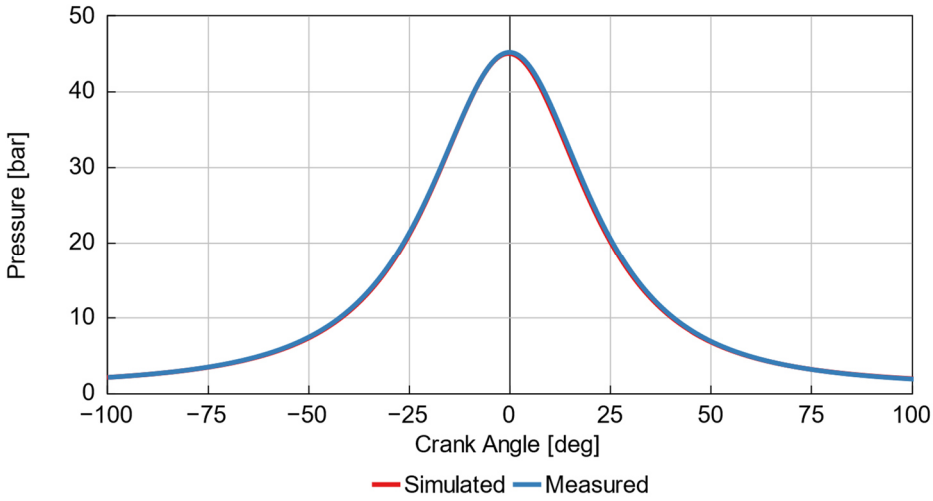

Figure 17: comparison of simulated and measured motoring curves at 1500 rpm and 1,3 bar charge air pressure

4.3. Cracker

Specifications

The cracker is developed under consideration of different boundary conditions. On the one hand, the catalyst sets a lower limit for the reaction temperature. Below this temperature, sufficient conversion is no longer achieved. The temperature has been determined in various catalyst tests. On the other hand, temperature limitations set by the material of the reactor wall are taken into account. Extensive literature research showed that the number of materials which meet the requirements set by temperature, pressure and the presence of ammonia and hydrogen is limited. However, one material could be identified that is certified for pressure applications (>500 mbar.g) and which shows promising results to withstand ammonia atmosphere up to 750 °C. This temperature limit is currently being verified by means of isothermal exposure tests in ammonia atmosphere at high temperature and high pressure including subsequent metallographic examinations. In addition to the temperature limits set by the catalyst and the reactor material the cracker has to fulfill the requirements set by the engine. The main requirements are summarized in Table 4. The Cracker hast to provide a hydrogen power of 150 kW_{H2} which corresponds to a hydrogen mass flow of 4.5 kg/h. The pressure of the product gas needs to be at least 8 bara. Moreover, it is desirable that the product temperature is below 60 °C and the residual ammonia content is less than 5 mol%. According to the requirements imposed by mobile application, a monolithic catalyst system is to be used.

Table 4: Boundary conditions for the development of the ammonia cracking plant

Description	**Value**
Hydrogen power of the cracker product gas	150 kW
Cracker product gas pressure	> 8 bara
Cracker product gas temperature	< 60 °C
Residual ammonia content of the cracker product gas	x_{NH3} < 5 mol% (corresponds to conversion > 90%)
Catalyst	Monolith

The heat required for the endothermic reaction is to be provided either by a) a hot gas generated by a gas burner or b) electrically, whereby the burner is to be operated with ammonia and a certain amount of the cracker product gas. Experiments at ZBT have shown that the combustion of a fuel with a composition of x_{NH3} = 40 mol%, x_{N2} = 15 mol% and

x_{H2} = 45 mol% has similar properties to the combustion of natural gas. Therefore, an ammonia content of 40 mol% is assumed.

Process development

A simplified flow diagram of the gas-heated process developed in Aspen Plus® is depicted in Figure 18. Ammonia is fed to the process as a gas (10 bar, 25 °C) and is preheated in a first heat exchanger (1) before being decomposed in the reactor (4). The product gas is then used to preheat the educt. A partial flow of the product gas is taken downstream of the first heat exchanger (1) and is fed to the burner (5) along with a second ammonia educt stream. In a second heat exchanger (2), the product gas is cooled to the required temperature of 60 °C, thereby preheating a secondary air stream. The temperature of the secondary air stream is further increased by the flue gas emitting the reactor in a third heat exchanger (3), thereby cooling down the exhaust gas. The preheated secondary air stream is used to control the flue gas temperature and, as the flue gas is used to heat the reactor, in the end to control the reaction temperature as well as the reactor wall temperature.

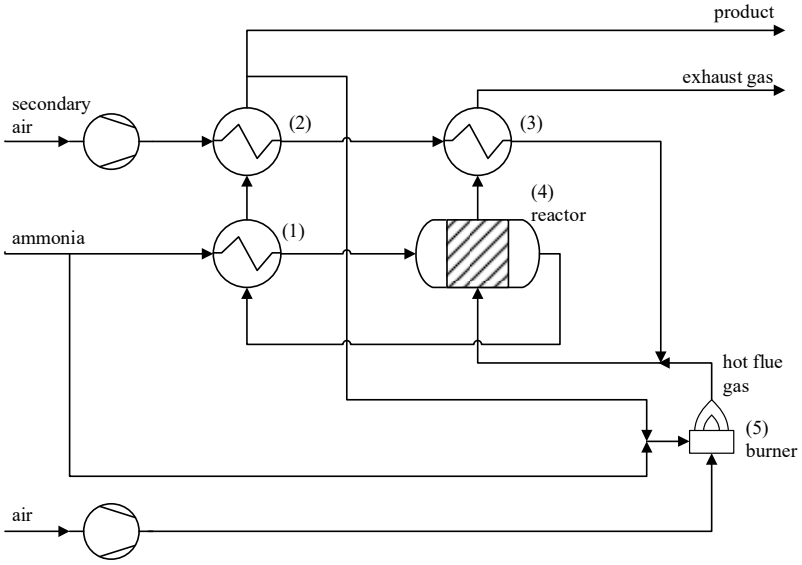

Figure 18: Simplified process flow diagram of the ammonia cracker

The amount of energy provided by the burner is 35 kW and the total amount of ammonia required is approximately 32 kg/h. The efficiency of the process is calculated according to equation (7) and is based on the lower heating value (H_L) and considers the energy required for compressors but neglects heat losses. In addition, since the system should be able to work autarkic on a ship, it is assumed that all electric energy consumed by the cracker system has to be produced by the GenSet with an efficiency of η_E = 38%. The compressor efficiency is conservatively estimated at η_C = 30%.

$$\eta_{Cr} = \frac{\dot{m}_{H2} \cdot H_{L_{H2}} + \dot{m}_{NH3} \cdot H_{L_{NH3}}}{(\dot{m}_{NH3B} + \dot{m}_{NH3C}) \cdot H_{L_{NH3}} + \frac{1}{\eta_C \cdot \eta_E} \cdot P_c} \tag{7}$$

For the given boundary conditions set by the engine, the wall material and the catalysts a maximum efficiency of 71% is achieved.

A simplified flow diagram of the electrically heated process is illustrated in Figure 19. Similar to the gas-heated process, ammonia is fed to the system at 25 °C and 10 bar and is preheated in a first heat exchanger (1). The preheated ammonia is decomposed in an electrically heated reactor (2). The hot product is used to preheat the ammonia feed. The product outlet temperature of 145 °C exceeds the limit of 60 °C so additional cooling is necessary. Since this system does not need a burner and a secondary air system it is much less complex. Also due

to the missing secondary air system no compressors are necessary which leads to an increased efficiency of up to 80%. Because of its lower complexity and higher efficiency compared to the gas heated process, the electrically heated system is being further developed. Based on the results of the process simulation, the components can be designed in detail in a following step.

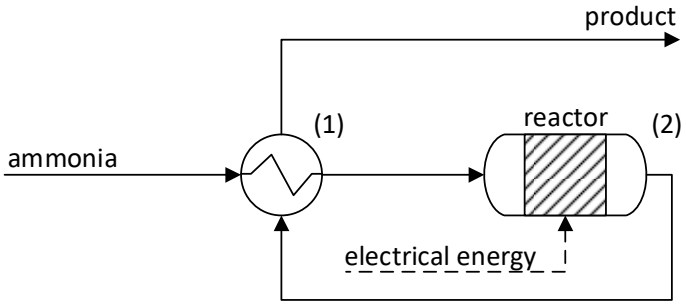

Figure 19: Simplified process flow diagram of the electrically heated ammonia cracker

5. Conclusion & Outlook

The pressing necessity of CO_2 emission reduction in all industries implies that solutions for the shipping branch must be developed as well with high priority. Beside others, green ammonia looks like a promising fuel for ships. Worldwide trading and handling of ammonia are already in place and ease the establishment of a respective marine fuel supply chain. Ammonia can act as an attractive hydrogen carrier because much less effort in transport and distribution in comparison to pure hydrogen is required. Production can happen at locations of renewable energy generation e.g. from solar, wind and hydropower.
In the presented project a maritime propulsion system is developed based on a new concept consisting of a pressurized ammonia cracker and a high-speed engine. The envisaged use case for this setup are vessels for inland water ways. Therefore, important topics are the system integration for future simple handling and the safety aspects to be considered on board. The technological aspects and challenges for establishing such a system were discussed in this paper. This includes especially the partly ammonia cracking towards hydrogen at engine boost pressure level as integral part of the combustion process as well as the impacts of ammonia on the engine setup and operation. By deepening the simulation tasks, fed by the results from systematic investigations on a single-cylinder engine, the complete process is optimized. This enables us to prepare the multi-cylinder engine by receiving the latest setup based on the final simulation and single-cylinder engine results.
As soon as the containerization of the multi-cylinder engine is finalized, the engine container is going to be tested at the CAMPFIRE Open Innovation Lab (COIL) near to Rostock/Germany. Later, this will be married with the ammonia cracker as completed system for initial and later endurance testing.

6. Acknowledgements

This work was carried out within the CAMPFIRE project of the Hydrogen Flagship Project TransHyDE and was funded by German Federal Ministry for Education and Research. Convergent Science provided CONVERGE licenses and technical support for this work. The authors acknowledge support by the state of Baden-Württemberg through bwHPC.

References

[1] Nathan Gray et al. “Decarbonising ships, planes and trucks: An analysis of suitable low-carbon fuels for the maritime, aviation and haulage sectors”. In: Advances in Applied Energy 1 (2021), p. 100008. ISSN: 26667924. DOI: 10.1016/j.adapen.2021.100008.

[2] J. Walter, M. Borning, and A. Moser. “Analyzing the Potential Production Amount of Synthetic Fuels in Germany”. In: 2021 IEEE Madrid PowerTech. IEEE, 2021, pp. 1–6. ISBN: 978-1-6654-3597-0. DOI: 10.1109/PowerTech46648.2021.9494888.

[3] Ghassan Chehade and Ibrahim Dincer. “Progress in green ammonia production as potentialcarbon-free fuel”. In: Fuel 299 (2021), p. 120845. ISNN: 0016-2361. DOI: 10.1016/j.fuel.2021.120845.

[4] Aaishi Ashirbad and Avinash Kumar Agarwal. “Scope and Limitations of Ammonia as Transport Fuel”. In: Greener and Scalable E-fuels for Decarbonization of Transport. Ed. by Avinash Kumar Agarwal and Hardikk Valera. Energy, Environment, and Sustainability. Singapore: Springer, 2022, pp. 391–418. ISBN: 978-981-16-8343-5. DOI: 10.1007/978-981-16-8344-214.

[5] Rachael H. Dolan, James E. Anderson, and Timothy J. Wallington. “Outlook for ammonia as a sustainable transportation fuel”. In: Sustainable Energy & Fuels 5.19 (2021), pp. 4830–4841. DOI: 10.1039/D1SE00979F.

[6] A. Feindt. Ammoniak in der Schifffahrt. Hamburg, 2023

[7] Hinrich Mohr. CAMPFIRE – Development of an Ammonia-fueled Cracker-Engine-Power Unit for Inland Waterway Shipping. Hamburg, Sept. 6, 2022.

[8] Sandra Tjaden. Struktur der deutschen Binnenschiffsflotte. Ed. by Wasserstraßen- und Schifffahrtsverwaltung des Bundes. Apr. 26, 2023. url: https://www.forschungsinformationssystem.de/servlet/is/123471/ visted at June 13, 2023.

[9] Volker Renner and Wolfgang Bialonski. “Technische und wirtschaftliche Konzepte für flußangepaßte Binnenschiffe”. In: Versuchsanstalt für Binnenschiffbau e.V., Duisburg 1701 (2004).

[10] Cecil E. Vanderzee und Delbert L King „The enthalpies of solution and formation of ammonia” The Journal of Chemical Thermodynamics 4(5):675-683, 1972.

[11] Jacob A. Mouljin et al. "Monolithic Catalysts and Reactors: High Precision with Low Energy Consumption" Advances in Catalysis Volume 54, Chapter 5 (2011)

[12] Zaev, I., Smirnov, S., and Gordeev, V., "Performance of the Mixture of Ammonia and Ammonia Decomposition Products as a Carbon-Free Fuel for Spark Ignition Engines," SAE Technical Paper 2023-01-1638, 2023, https://doi.org/10.4271/2023-01-1638. Peoples Friendship University of Russia

[13] Pessina, V.; Berni, F.; Fontanesi, S.; Stagni, A.; Mehl, M. (2022): Laminar flame speed correlations of ammonia/hydrogen mixtures at high pressure and temperature for combustion modeling applications. In: International Journal of Hydrogen Energy 47 (61), S. 25780–25794. DOI: 10.1016/j.ijhydene.2022.06.007

[14] Basshuysen, R. v.; Schäfer, F. (2015): Handbuch Verbrennungsmotoren. Wiesbaden, S.487 DOI: 10.1007/978-3-658-04678-1

[15] GAMMA TECHNOLOGIES: Engine Performance Application Manual: Version 2022. S.20